2008 American Control Conference
Westin Seattle Hotel, Seattle, Washington, USA
June 11-13, 2008

Modelling and Control of a Miniature Ducted-Fan in Fast Forward Flight

R. Naldi, L. Marconi and A. Sala

Center for research on complex Automated SYstems (CASY)
DEIS-University of Bologna, ITALY.

Abstract— **In this paper we present both the modelling and preliminary control results relative to a configuration of ducted-fan MAV (Miniature Aerial Vehicle) which is characterized by a mechanical and aerodynamical structure designed in order to allow efficient forward flights at small values of the angle of attack. Thanks to these modifications the system is able to accomplish both stationary and fast forward flight by means of a transition between two different operative configurations. After deriving a nonlinear model capable to describe the system dynamics in a general flight envelope, which include slow flights, fast forward flights at low values of angle of attack and the transition between the two previous conditions, we concentrate on the fast forward flight presenting preliminary control results.**

I. INTRODUCTION

Recent applications of both civil and military UAVs show the effectiveness of VTOL configuration in succeeding in a large variety of tasks, such as, besides others, surveillance, image acquisition, enemy detection, etc. (see [1]). Helicopters, ducted-fan and four rotor UAVs are examples of vehicles adopted to cover these applications. A problem that commonly affects these systems is the limitation in obtaining reasonably fast forward flight without consuming a large amount of the onboard energy. In fact all these VTOL configurations have to compensate for the gravity force through the main thrust generated by the rotor disc or the propeller and present a forward motion characterized by high drag coefficient value due to their particular shape. This problem can be overcome by adopting configurations able to fly like airplanes during the fast forward flight. These configurations are able to use the aerodynamic lift forces generated by proper aerodynamic surfaces in order to compensate for the gravity, reducing the overall amount of energy necessary to maintain the vehicle over the desired flight path. Inspired by these considerations, we focus on the ducted-fan aerial vehicle presented in [2] whose aerodynamical design has been suitably modified to allow for fast forward flights with small angles of attach. In particular the ducted-fan that we are presenting is able to change its attitude at a certain speed in order to use the duct itself and other fixed aerodynamic surfaces as wings to let the system fly almost as efficiently as a standard airplane. The change of configuration, which let the system to achieve really small values of angle of attack, allow also to reduce significatively the overall drag force.

This work was supported by MIUR. Corresponding author: Roberto Naldi, CASY-DEIS University of Bologna, Via Risorgimento 2, 40136 Bologna, Italy. Tel: 0039 051 2093788, Fax: 0039 051 2093073, email: roberto.naldi@unibo.it

As a main contribution in this work we provide a nonlinear dynamical model of the system which is able to describe stationary flight, fast forward flight and the transitions between the two flight conditions. This model, in future work, will allow the design of control laws which stabilize system dynamics in all flight conditions. The emphasis of this preliminary work, with respect to recent contributions focusing on control of ducted-fan miniature vehicles in case of low speed or hovering flight (see for example [3]), is on the analysis of the second scenario, in which the system is flying at a certain reasonably high speed. For this particular scenario we provide an analysis of a desired trim trajectory and a simplified linear model useful for preliminary control design by means of linear techniques. In order to stabilize the vehicle over the desired trim trajectory, taking advantage of the linear model previously derived, we design a linear ”frequency shaped” optimal control law.

The paper is structured as follow. Section II analyzes the forces and torques acting on the system in case of a general flight. Section III focuses the analysis to the case of forward flight at low values of angle of attack, providing a simplified nonlinear model for the system and a first order linear approximation for control purpose. Section IV presents the synthesis of a linear optimal controller and simulation results to show the effectiveness of the proposed results.

Notation - We use the compact notation C_a, S_a, T_a with $a \in I\!R$ to denote respectively $\cos a$, $\sin a$ and $\tan a$. For a vector $\omega = col(\omega_1, \omega_2, \omega_3)$, Skew($\omega$) denoted the 3×3 skew-symmetric matrix with the first, second and third row respectively given by $[0, -\omega_3, \omega_2]$, $[\omega_3, 0, -\omega_1]$ and $[-\omega_2, \omega_1, 0]$, I denotes the 3×3 identity matrix.

II. ANALYSIS OF THE FORCES AND TORQUES ACTING ON THE VEHICLE

The ducted-fan MAV that we are considering can be thought as divided into three different subsystems (see [2] and Figure 1). The first subsystem is represented by a fixed pitch propeller connected to an electric motor. This subsystem is in charge of generating the necessary thrust in order to actuate the overall vehicle. The second subsystem is composed by a set of active flaps necessary to achieve full authority control of vehicle’s attitude. Finally the third subsystem is composed by the fixed aerodynamic surfaces, in particular the duct itself, which is designed to protect the environment from the propeller and to improve the efficiency of thrust's generation mechanism, and a set of fixed wings which are collocated on the vehicle in order to augment the overall lift force during high speed flight and to balance the overall momentum like it happens in standard airplanes.

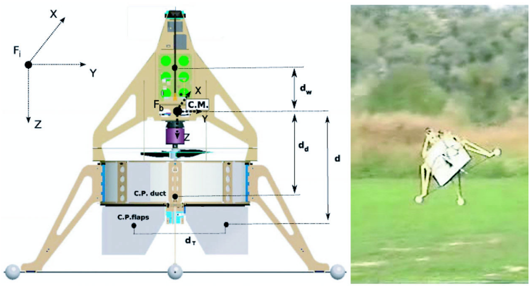

Fig. 1. The ducted-fan Micro Aerial Vehicle.

A mathematical model for the system could be derived making use of Newton-Euler equations of motion of a rigid body in the configuration space $SE(3) = I\!R^3 \times SO(3)$. By considering an inertial coordinate frame $F_i = \{O_i, \overrightarrow{i}_i, \overrightarrow{j}_i, \overrightarrow{k}_i\}$ and a coordinate frame $F_b = \{O_b, \overrightarrow{i}_b, \overrightarrow{j}_b, \overrightarrow{k}_b\}$ attached to the body, the model of the MAV with respect to the inertial frame could be written as follow

$$\begin{array}{rcl} m\ddot{p}^i & = & R_{ib} f^b \\ J\dot{\omega}^b & = & -\text{Skew}(\omega^b)J\omega^b + w_e G\omega^b + \tau^b \end{array} \quad (1)$$

where f^b and τ^b represents respectively the vector of forces and torques applied to the vehicle expressed in the body frame, m the vehicle total mass, $J = diag(J_x, J_y, J_z)$ the diagonal inertia matrix, $p^i = \text{col}(x^i, y^i, z^i)$ the position of the center of mass expressed in the inertial frame, ω^b the angular velocity expressed in the body frame, R_{ib} the rotation matrix relating the two reference frames. G is the skew symmetric matrix $\text{Skew}(col(0, 0, I_{rot}))$ where $I_{rot} \in I\!R^+$ is the inertia of the propeller with respect to the spin axis. Term $w_e G\omega$ in (1) models the gyroscopic precession torque effect of the rotating fan.

To avoid singularities in the description of system dynamics both in stationary and in fast forward flight rotation matrix R_{ib} has been parameterized by means of unit quaternion $\mathbf{q} = (q_0, q) \in I\!R^4$, where q_0 and $q = (q_1, q_2, q_3)^T$ denote respectively the scalar and the vector part, satisfying the constraint $q_0^2 + \|q\|^2 = 1$. Accordingly R_{ib} is given by

$$R_{ib} = \begin{pmatrix} 1 - 2q_2^2 - 2q_3^2 & 2q_1q_2 - 2q_0q_3 & 2q_1q_3 + 2q_0q_2 \\ 2q_1q_2 + 2q_0q_3 & 1 - 2q_1^2 - 2q_3^2 & 2q_2q_3 - 2q_0q_1 \\ 2q_1q_3 - 2q_0q_2 & 2q_2q_3 + 2q_0q_1 & 1 - 2q_1^2 - 2q_2^2 \end{pmatrix}$$

and the cinematic equations are given by the following so-called quaternion propagation equation

$$\dot{\mathbf{q}} = \frac{1}{2}E(\mathbf{q})\omega \quad (2)$$

in which

$$E(\mathbf{q}) = \begin{pmatrix} -q^T \\ q_0 I + \text{Skew}(q) \end{pmatrix}.$$

A. Aerodynamic Simplifications

To model forces and torques generation mechanisms simple aerodynamic arguments are used. For an airfoil profile with area S moving into air with relative wind velocity V, the lift and the drag forces (see [4]) are given respectively by

$$L = \frac{1}{2}\rho V^2 C_L(\alpha) S \quad D = \frac{1}{2}\rho V^2 C_R(\alpha) S \quad (3)$$

where ρ is air density and $C_L(\alpha)$, $C_D(\alpha)$ are respectively the lift and drag coefficients which depend on the angle of attack α with respect to relative wind. In case of airfoil profiles characterized by small Reynolds numbers and assuming reasonably small angles of attack, it is possible to consider the following simplified expressions

$$C_L(\alpha) = c_L\alpha \quad C_D(\alpha) = c_D\alpha^2 \quad (4)$$

where c_L and c_D are constant coefficients. As far as the external disturbances are concerned we model wind velocity $\dot{p}_w$ in the inertial frame as

$$\dot{p}_w^i = \begin{pmatrix} \dot{x}_w^i \\ \dot{y}_w^i \\ \dot{z}_w^i \end{pmatrix}$$

The relative wind vector $r_w \in I\!R^3$ in the inertial frame is then given by the following expression

$$r_w^i = \dot{p}_w^i - \dot{p}^i \quad (5)$$

where the second term indicates the relative wind induced by the forward speed of the aircraft. For medium to high translational speed we assume that the magnitude of $\dot{p}_w^i$ is negligible compared to the magnitude of $\dot{p}^i$.
The relative wind vector measured in the center of mass in the body frame is given by $r_w^b = R_{ib}^T r_w^i$. As an approximation we assume that the above expressions continues to hold for all points belonging to the rigid body (i.e. we neglect any aerodynamic effects due to angular velocity of the rigid body). To simplify the notation, in the computation of the aerodynamic pressure, we denote with V the module of the relative wind $\|r_w\|$ which is invariant in all reference frames.

B. Thrust Generation Subsystem

The modeling of the propeller subsystem can be done accordingly to classical disc actuator theory or blade element theory (see references [5], [6] and [7] for more details). In order to simplify the thrust model, we approximate the propeller thrust T and resistant torque Q assuming only forward motion of the propeller for Mach number $M << 1$ obtaining

$$\begin{array}{rcl} T(r_{w_z}^b, w_e) & = & c_T\left(1 - \text{atan}\left(r_{w_z}^b, w_e\right)\right) w_e^2 \\ Q(r_{w_z}^b, w_e) & = & c_Q\left(1 - \text{atan}\left(r_{w_z}^b, l_p w_e\right)\right) w_e^2 \end{array} \quad (6)$$

in which c_T, c_Q are constant parameters which depends on local air density and l_p is a constant parameter which depends on the geometry of the propeller. Output velocity of the air generated by the propeller, denoted by v_{induced} is approximated by the following expression

$$v_{\text{induced}} = c_{\text{i}}\sqrt{T}\,. \tag{7}$$

with c_{i} a positive constant. Observe that the output velocity represents also one of the components of the relative wind velocity in the computation of the forces generated by each active flap. In particular if we concentrate the analysis to the case of low speed flight, this component represent the overall relative wind in order to actuate the system through the set of active flaps.

C. Flaps Subsystem

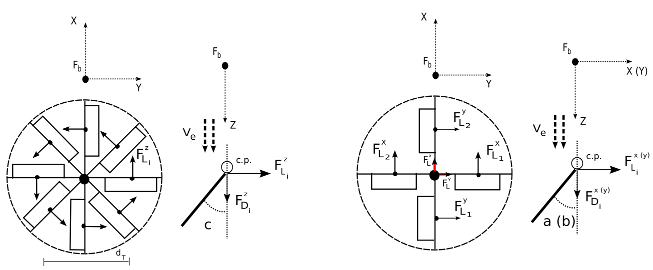

Fig. 2. Flaps subsystems: anti-torque and lateral/longitudinal flaps.

To obtain full controllability of the attitude dynamics a set of active flaps have been positioned below the propeller in order to deviate the air flow. A first level of flaps is responsible of controlling the *yaw* attitude dynamics, counteracting the engine torque, whereas a second level is in charge of controlling both the *roll* and *pitch* attitude dynamics. We assume that effective wind velocity V_{e} normal to the propeller disc is given by $V_{\text{e}} = v_{\text{induced}} + r^b_{w_z}$. With an eye at (3), (4) and at figure 2 it is possible to write the expressions of the resultant forces along body frame axis as

$$\begin{array}{rclcl} F_L \cdot \overrightarrow{i}_b &=& \sum_i F^x_{L_i} &=& c_{L_F}\cdot a \cdot V_{\text{e}}^2 \\ F_L \cdot \overrightarrow{j}_b &=& \sum_i F^y_{L_i} &=& c_{L_F}\cdot b \cdot V_{\text{e}}^2 \\ F_L \cdot \overrightarrow{k}_b &=& \sum_i F^z_{L_i} &=& 0 \end{array} \tag{8}$$

$$\begin{array}{rcl} F_D \cdot \overrightarrow{k}_b &=& \sum_{j=\{x,y,z\}} \sum_i F^j_{D_i} \\ &=& [k_{D_F}\cdot(a^2+b^2) + k_{D_Z}\cdot c^2]\cdot V_{\text{e}}^2 \end{array}$$

in which c_{L_F}, k_{D_F} and k_{D_Z} are constant parameters, c represent the angle of attack of the flaps positioned in the first level and a, b the angles of attack of the flaps positioned in the second level respectively along the lateral y axis and along the longitudinal x axis. The effects of the forces on the rigid body can be calculated considering F^x_L and F^y_L applied at a distance d from the center of mass, as shown in figure 1, and the points of application of any two opposite flaps belonging to the anti-torque subsystem at a distance d_T. The torque vector τ_{flaps} is then given by

$$\tau^b_{\text{flaps}} = A(V_{\text{e}}^2)v \tag{9}$$

with

$$v = \text{col}(a,\, b,\, c) \tag{10}$$

and with

$$A(V_{\text{e}}^2) = V_{\text{e}}^2 \begin{pmatrix} 0 & -c_1 & 0 \\ c_1 & 0 & 0 \\ 0 & 0 & -c_2 \end{pmatrix} \tag{11}$$

with $c_1 = C_{L_F} d$ and $c_2 = 2C^z_{L_F} d_T$, where the coefficient $C^z_{L_F}$ depends in the geometry of anti-torque flaps.

D. The Fixed Wings, the Duct and the Fuselage

In case of forward flight when the relative wind (5) assumes significative values it is necessary to take into account for the aerodynamic effects of all the aerodynamic surfaces. According to [7] the angle of attach $\alpha(r^b_w)$ and the sideslip angle $\beta(r^b_w)$ which model the relative incidence of the vehicle with respect to the relative wind are given by the following expressions

$$\begin{array}{rcl} \alpha(r^b_w) &=& \tan^{-1}\left(\dfrac{-r^b_{w_x}}{r^b_{w_z}}\right) \\ \beta(r^b_w) &=& \sin^{-1}\left(\dfrac{-r^b_{w_y}}{V}\right) \end{array} \tag{12}$$

Consider now the so-called wind frame $F_w = \{O_b,\, \overrightarrow{i}_w,\, \overrightarrow{j}_w,\, \overrightarrow{k}_w\}$ which is, by definition, related to the body frame by the following rotation matrix

$$R_{wb} = \begin{pmatrix} C_\alpha & S_\alpha S_\beta & S_\alpha C_\beta \\ 0 & C_\beta & -S_\beta \\ -S_\alpha & C_\alpha S_\beta & C_\alpha C_\beta \end{pmatrix}. \tag{13}$$

In this frame the aerodynamic forces of the wings, f^w_{wing}, of the duct, f^w_{duct}, and of other non profiled surfaces as the fuselage and the landing gear, f^w_{wing} have the following expression

$$f^w_{\text{aero}} = f^w_{\text{wing}} + f^w_{\text{duct}} + f^w_{\text{fus}} = \begin{pmatrix} -L_{\text{wing}} - L_{\text{duct}} \\ -S_{\text{duct}} \\ D_{\text{wing}} + D_{\text{duct}} + D_{\text{fus}} \end{pmatrix} \tag{14}$$

where L_{wing} and D_{wing} denote respectively the lift and drag forces relative to the fixed wings (see also figure 1), L_{duct}, S_{duct} and D_{duct} the lift, side and drag forces associated to the duct airfoil and D_{fus} the drag associated to the fuselage and other non profiled surfaces.

E. Momentum Drag

In presence of crosswind the vehicle must supply a force to align the incoming air flow with the duct. According to [5] and [6] this force can be written as

$$f^b_{\text{md}} = c_{\text{fd}} v_{\text{induced}} \begin{pmatrix} r^b_{w_x} \\ r^b_{w_y} \\ 0 \end{pmatrix}$$

The crosswind also cause a difference of pressure on the propeller disc which cause a momentum approximated as

$$\tau^b_{\text{md}} = c_{\text{md}} \begin{pmatrix} -r^b_{w_y}\|r^b_{w_y}\| \\ r^b_{w_x}\|r^b_{w_x}\| \\ 0 \end{pmatrix}$$

III. ANALYSIS OF HIGH SPEED FLIGHT AT LOW VALUES OF ANGLE OF ATTACK

The overall dynamical model of the system is a $12th$ order system described by rigid body equations (1) and (2) with a vector wrench given by all contributions described in the previous section II. The dynamics of the system are indeed driven by the three control inputs a, b, c and the angular rotor velocity w_{e}. All the aerodynamic forces have been introduced as external nonlinear forces which depend on the particular flying envelope of the vehicle. This model is sufficiently general to describe the vehicle in different flight conditions including both the stationary and, in particular, the fast forward flight. In order to deal with the last kind of flight condition we consider a desired nominal trajectory for the ducted-fan MAV which is given in the inertial frame as a constant speed along the x axis

$$\dot{p}^i = col(\bar{V}, 0, 0) \tag{15}$$

with $\bar{V}$ representing a positive constant velocity compatible with system dynamics. In order to synthesize a controller to stabilize the system over this kind of trajectories we introduce first some simplifications in the equations governing the system dynamics. We assume first that the angle of attack α is small enough so that the inflow is almost perpendicular to the propeller disc plane neglecting the momentum drag effects. For the same approximation the normal airflow component for the computation of propeller thrust T and torque Q is approximated as $r^b_{w_z} \approx \bar{V}$. The effective wind velocity V_{e}, the propeller thrust and the propeller torque have been simplified as follow

$$\begin{array}{rcl} V_{\mathrm{e}}(w_{\mathrm{e}}, \bar{V})^2 & = & k_{v_e}(\bar{V}) w_{\mathrm{e}} + \bar{V} \quad T(w_{\mathrm{e}}, \bar{V}) = k_T(\bar{V}) w_{\mathrm{e}}^2 \\ Q(w_{\mathrm{e}}, \bar{V}) & = & k_Q(\bar{V}) w_{\mathrm{e}}^2 \end{array} \tag{16}$$

in which

$$\begin{array}{rcl} k_T(\bar{V}) & = & c_T \left(1 - \dfrac{\bar{V}}{l_p \bar{w}_{\mathrm{e}}}\right) \quad k_Q(\bar{V}) = c_Q \left(1 - \dfrac{\bar{V}}{l_p \bar{w}_{\mathrm{e}}}\right) \\ k_{v_e}(\bar{V}) & = & c_i \sqrt{k_T(\bar{V})} \end{array}$$

Since in fast forward flight the angle β is also small it is possible to consider the approximations $C_\alpha \approx 1$, $S_\alpha \approx \alpha$, $C_\beta \approx 1$, $S_\beta \approx \beta$ and according to the definitions in (6)

$$\alpha = \mathrm{atan}\frac{-\dot{x}^b}{\dot{z}^b} \approx \frac{-\dot{x}^b}{\dot{z}^b} \quad \beta = \mathrm{asin}\frac{-\dot{y}^b}{\|\dot{p}^b\|} \approx \frac{-\dot{y}^b}{\dot{z}^b}\,.$$

This makes it possible to simplify the rotation matrix in (13) as

$$R_{bw} = \begin{pmatrix} 1 & 0 & -\alpha \\ \alpha\beta & 1 & \beta \\ \alpha & -\beta & 1 \end{pmatrix}. \tag{17}$$

The aerodynamic forces in (14) can be rewritten according to the approximations introduced in (4) as

$$f^w_{\mathrm{aero}} = \begin{pmatrix} -L(\alpha, \dot{p}^i) \\ -S(\beta, \dot{p}^i) \\ D_\alpha(\alpha, \dot{p}^i) + D_\beta(\beta, \dot{p}^i) + D_{\mathrm{fus}}(\dot{p}^i) \end{pmatrix} \tag{18}$$

in which

$$\begin{array}{ll} L(\alpha, \dot{p}^i) = c_{\mathrm{lift}}(\dot{p}^T \dot{p})\alpha & S(\beta, \dot{p}^i) = c_{L_{\mathrm{duct}}}(\dot{p}^T \dot{p})\beta \\ D_\alpha(\alpha, \dot{p}^i) = c_{\mathrm{drag}}(\dot{p}^T \dot{p})\alpha^2 & D_\beta(\beta, \dot{p}^i) = c_{D_{\mathrm{duct}}}(\dot{p}^T \dot{p})\beta^2 \\ D_{\mathrm{fus}}(\dot{p}^i) = c_{\mathrm{fus}}(\dot{p}^T \dot{p})\,. & \end{array}$$

with $c_{\mathrm{lift}} = c_{L_{\mathrm{duct}}} + c_{L_{\mathrm{wing}}}$ and $c_{\mathrm{drag}} = c_{D_{\mathrm{duct}}} + c_{D_{\mathrm{wing}}}$. To compute the resultant torque generated by the aerodynamic forces we consider each force applied in its center of pressure obtaining

$$\tau_{\mathrm{aero}} = \begin{pmatrix} c_{\tau_s} \\ 0 \\ 0 \end{pmatrix} (\dot{p}^T \dot{p})\beta \tag{19}$$

in which $c_{\tau_s} = -c_{L_{\mathrm{duct}}} d_d$. Observe that as a design constraint no significant torque contribution due to the lift force of the duct and of the main wing is taken into account since we assume that the vehicle is designed to have balanced pitching momentum for small angles of attack. Also torque effects of the drag forces are considered of second order.

The overall nonlinear external wrench vector that governs the dynamics in case of high speed flight is given as follow

$$\begin{array}{rcl} f^b & = & \begin{pmatrix} c_{L_F} a (k_{v_e} w_{\mathrm{e}} + \bar{V})^2 \\ c_{L_F} b (k_{v_e} w_{\mathrm{e}} + \bar{V})^2 \\ -k_T w_{\mathrm{e}}^2 \end{pmatrix} + R_{bw} f^w_{\mathrm{aero}} + \\ & + & R_{bi} \begin{pmatrix} 0 \\ 0 \\ mg \end{pmatrix} \\ \tau^b & = & (k_{v_e} w_{\mathrm{e}} + \bar{V})^2 \begin{pmatrix} 0 & -c_1 & 0 \\ c_1 & 0 & 0 \\ 0 & 0 & -c_2 \end{pmatrix} \begin{pmatrix} a \\ b \\ c \end{pmatrix} + \\ & + & \begin{pmatrix} 0 \\ 0 \\ k_Q \end{pmatrix} w_{\mathrm{e}}^2 + \tau_{\mathrm{aero}}\,. \end{array} \tag{20}$$

A. Linear Approximation of Forward Flight Dynamics

In order to simplify the synthesis of a controller for the forward flight, we consider in this section a linear approximation of the dynamics of the systems. The forward motion trajectory (15) is characterized by the following unit quaternion

$$\bar{\mathbf{q}} = \begin{pmatrix} \bar{q}_0 = C_{\frac{-(\pi/2 - \bar{\alpha})}{2}} \\ 0 \\ \bar{q}_2 = S_{\frac{-(\pi/2 - \bar{\alpha})}{2}} \\ 0 \end{pmatrix}. \tag{21}$$

With an eye at (20) the four control inputs necessary to maintain the system's dynamics over the desired trajectory are

$$\begin{array}{rcl} \bar{a} & = & \bar{b} = 0 \\ \bar{c} & = & \dfrac{k_Q \bar{w}_{\mathrm{e}}^2}{c_2 (k_{v_e} \bar{w}_{\mathrm{e}} + \bar{V})^2} \\ \bar{w}_{\mathrm{e}}^2 & = & \dfrac{C_{\mathrm{drag}} \bar{V}^2 \bar{\alpha}^2 + c_{\mathrm{fus}} \bar{V}^2}{k_T} \end{array} \tag{22}$$

and the angle of attack $\bar{\alpha}$ is given by the unique real and positive solution of the equation

$$C_{\mathrm{drag}} \bar{\alpha}^3 + (c_{\mathrm{lift}} + c_{\mathrm{fus}})\bar{\alpha} = \frac{mg}{\bar{V}^2}$$

Finally the sideslip angle $\beta = 0$. Neglecting higher order terms, the linear model of the ducted-fan MAV for fast forward flight is given by the following linear system with state (omitting the superscript ^{i}) $x = col(\delta x, \delta \dot{x}, \delta y, \delta \dot{y}, \delta z, \delta \dot{z}, \delta q_0, \delta q_1 \delta \dot{q}_2, \delta q_3, \delta \omega_x, \delta \omega_y, \delta \omega_z)$ and inputs $u = col(\delta a, \delta b, \delta c, \delta w_{\mathrm{e}})$

$$
\begin{aligned}
m\delta\ddot{x} &= c_{\mathrm{lift}}\bar{V}^2\bar{\alpha}\left(4\bar{q}_2\delta q_2 - 2\bar{q}_0\bar{\alpha}\delta q_2 - 2\bar{q}_2\bar{\alpha}\delta q_0\right) + \\
&+ c_{L_F}\bar{\alpha}(k_{v_e}\bar{w}_{\mathrm{e}} + \bar{V})^2\delta a + \\
&- 2\bar{V}\left(2c_{\mathrm{drag}}\bar{\alpha}^2 + c_{\mathrm{fus}}\right)\delta\dot{x} + \\
&+ 2k_T\bar{w}_{\mathrm{e}}\delta w_{\mathrm{e}} + \bar{V}^2\bar{\alpha}\left(c_{\mathrm{lift}} - 2c_{\mathrm{drag}}\right)\delta\alpha \\
m\delta\ddot{y} &= -2c_{\mathrm{lift}}\bar{V}^2\bar{\alpha}\left(\bar{q}_2 - \bar{q}_0\bar{\alpha}\right)\delta q_1 + \\
&- 2c_{\mathrm{lift}}\bar{V}^2\bar{\alpha}\left(\bar{q}_0 + \bar{q}_2\bar{\alpha}\right)\delta q_3 + \\
&+ c_{L_F}(k_{v_e}\bar{w}_{\mathrm{e}} + \bar{V})^2\delta b - c_{L_{\mathrm{duct}}}\bar{V}^2\delta\beta \\
m\delta\ddot{z} &= c_{\mathrm{lift}}\bar{V}^2\bar{\alpha}\left[2\bar{q}_2\delta q_0 + (2\bar{q}_0 + 4\bar{q}_2\bar{\alpha})\delta q_2\right] + \\
&+ c_{L_F}(k_{v_e}\bar{w}_{\mathrm{e}} + \bar{V})^2\delta a - 2c_{\mathrm{lift}}\bar{V}\bar{\alpha}\delta\dot{x} + \\
&- c_{\mathrm{lift}}\bar{V}^2\delta\alpha \\
J_x\delta\dot{w}_x &= -I_r\bar{w}_{\mathrm{e}}\delta w_y - c_1(k_{v_e}\bar{w}_{\mathrm{e}} + \bar{V})^2\delta b + c_{\tau_s}\bar{V}^2\delta\beta \\
J_y\delta\dot{w}_y &= I_r\bar{w}_{\mathrm{e}}\delta w_x + c_1(k_{v_e}\bar{w}_{\mathrm{e}} + \bar{V})^2\delta a \\
J_z\delta\dot{w}_z &= -c_2(k_{v_e}\bar{w}_{\mathrm{e}} + \bar{V})^2\delta c + \frac{2k_Q\bar{V}\bar{w}_{\mathrm{e}}}{k_{v_e}\bar{w}_{\mathrm{e}} + \bar{V}}\delta w_{\mathrm{e}}
\end{aligned}
\tag{23}
$$

where

$$
\begin{aligned}
\delta\alpha &= \frac{1 + \bar{\alpha}^2}{\bar{V}}\delta\dot{z} + 2\bar{q}_2\bar{\alpha}\delta q_0 - (4\bar{q}_2 - 2\bar{q}_0\bar{\alpha})\delta q_2 \\
\delta\beta &= \frac{1}{\bar{V}}\delta\dot{y} + 2\bar{q}_2\delta q_1 - 2\bar{q}_0\delta q_3
\end{aligned}
$$

and with

$$
\begin{pmatrix} \delta\dot{q}_0 \\ \delta\dot{q}_1 \\ \delta\dot{q}_2 \\ \delta\dot{q}_3 \end{pmatrix} = \frac{1}{2}\begin{pmatrix} 0 & -\bar{q}_2 & 0 \\ \bar{q}_0 & 0 & \bar{q}_2 \\ 0 & \bar{q}_0 & 0 \\ -\bar{q}_2 & 0 & \bar{q}_0 \end{pmatrix}\begin{pmatrix} \delta w_x \\ \delta w_y \\ \delta w_z \end{pmatrix}.
$$

IV. DESIGN OF THE CONTROL LAW

In order to stabilize the system over the desired trajectory, taking advantage of the linear approximated model previously derived, we consider a linear optimal controller with integral action on the lateral and vertical position in order to obtain asymptotic robustness to constant external disturbances such as small constant wind disturbances (readers are referred to [8] and [9] for more details about the following linear control techniques). To this purpose we chose to minimize the following integral cost function

$$
J = \frac{1}{4\pi}\int_{-\infty}^{+\infty}\hat{X}(jw)^T\hat{Q}(jw)\hat{X}(jw)dw
$$

in which $\hat{X}(jw) = \left[\begin{array}{cc} X(jw) & U(jw) \end{array}\right]$ and

$$
\hat{Q}(jw) = \left[\begin{array}{cc} Q(jw) & 0 \\ 0 & R(jw) \end{array}\right]
$$

where $X(jw)$ and $U(jw)$ denotes Fourier transforms of respectively $x(t)$ and $u(t)$, $R(jw)$ is chosen as the following diagonal real matrix

$$
R(jw) = diag\left\{\frac{1}{J_y^2}, \frac{1}{J_x^2}, \frac{1}{J_z^2}, \frac{1}{m^2}\right\}
$$

TABLE I

PARAMETERS OF THE DUCTED-FAN MAV

$m = 1.286\ kg\ ,\ J = diag(1.8, 1.7, 0.8)\ 10^{-2}\ kg \cdot m$
$d, d_d, d_T, d_{w1}, d_{w_2}, l_p = 0.19, 0.10, 0.16, -0.05, -0.16, 0.1\ m$
$c_{L_F}, c_{L_F}^z, c_{L_{\mathrm{duct}}} = 0.0486, 0.028, 0.2\ Kg \cdot m/rad$
$c_{L^1_{\mathrm{wing}}}, c_{L^2_{\mathrm{wing}}} = 0.18, 0.068\ Kg \cdot m/rad$
$c_{D_{\mathrm{wing}}}, c_{\mathrm{fus}}, c_{D_{\mathrm{duct}}} = 0.15, 0.004, 0.20\ N/(mrad^2)$
$c_T = 1.02 \cdot 10^{-5}\ N/rad^2\ ,\ c_i = 2.60\ m/(s \cdot sqrtN)$
$c_{\mathrm{fd}} = 0.02\ N \cdot s/m$
$V = 15\ m/s\ ,\ \bar{w}_{\mathrm{e}} = 445\ rad/s$
$\bar{\alpha} = 0.12\ rad, ,\ \bar{a} = b = \beta = 0\ rad\ ,\ \bar{c} = 0.0062\ rad$
$a_z, b_z, c_z = 0.0244, -0.0023, 5.7220 \cdot 10^{-5}$

whereas the matrix $Q(jw)$ is chosen as

$$
Q(jw) = diag\left\{q_i\right\}, \quad i \in \{1, 12\}
$$

with $q_i = 1/\omega^2$ for $i = 3, 5$ (corresponding the the y and z state variable) and $q_i = 1$ otherwise. To avoid eigenvalues closed to the imaginary axis we impose also a stability margin $\gamma = 0.3$ in order to have

$$
\lim_{t \mapsto \infty}\frac{\|x(t)\|}{e^{-\gamma t}} < +\infty .
$$

In order to test the controller we consider the following trajectory which corresponds to a forward ascending trajectory with

$$
\begin{aligned}
x^\star(t) &= \bar{V}t \\
y^\star(t) &= 0 \\
z^\star(t) &= a_z \cdot t^3 + b_z \cdot t^4 + c_z \cdot t^5 .
\end{aligned}
\tag{24}
$$

with initial conditions $y(0) = -0.6\ m$, $z(0) = 0.2\ m$ and $\dot{x}(0) = 14.5\ m/s$. A constant wind disturbance $w^i_{\mathrm{wind}} = (0, -0.3, 0)\ m/s$ is considered from time $t = 20$. Despite the presence of this disturbance, which effect is visible in the y inertial coordinate in figures 3 and 4, the closed-loop system is able to achieve small asymptotic error and in particular the y and z positions, converge to the desired one thanks to the integral action embedded in the control law. Figure 4 shows the velocity trajectory of the system. Even in this case observe that after a transient the ducted-fan recovers the default trajectory (15). Figures 5 and 6 show respectively the flight path angles (see [7]), the angle of attack and the sideslip angle. Observe that during the transient both bank and the sideslip angles are used in order to displace the vehicle. This happens because with the particular annular fuselage of the MAV the side force is relevant and can be used to govern the lateral dynamics. Observe also that the angle of attack α acts as a virtual control input for the vertical dynamics in order to increase the lift during the first part of the transient to let the system reach the desired altitude. Finally the four control inputs are shown in figure 7.

V. CONCLUSIONS

In this paper we presented the modelling of a particular configuration of ducted-fan MAV in case of a general flight envelope that include in particular high speed flight at low values of angles of attack. By means of a linear approximation of system dynamics we also design a linear optimal

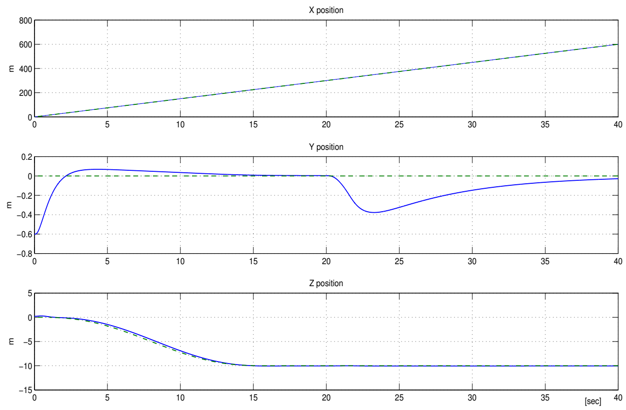

Fig. 3. Position x^i, y^i and z^i (solid lines) with respect to the referenc trajectories (dash-dotted lines).

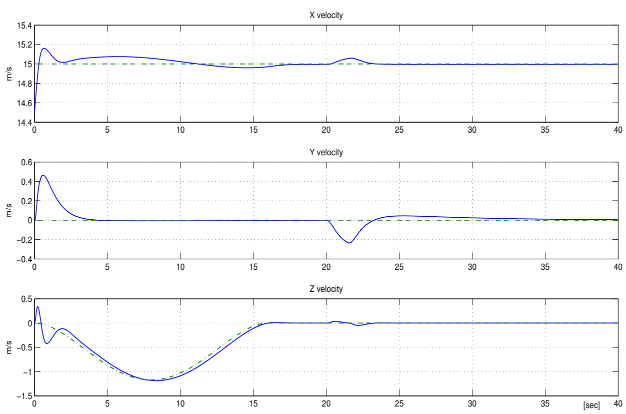

Fig. 4. Velocity x^i, y^i and z^i (solid lines) with respect to the reference trajectories (dash-dotted lines).

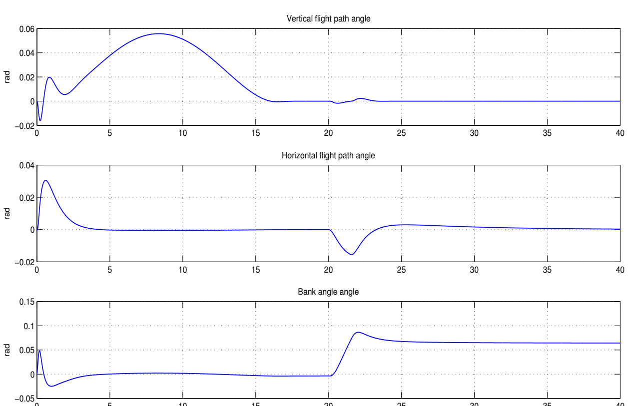

Fig. 5. The vertical flight path angle γ, the horizontal flight path angle ξ and the bank angle μ.

controller to stabilize the system over a particular high speed trajectory despite the presence of small disturbances. Future

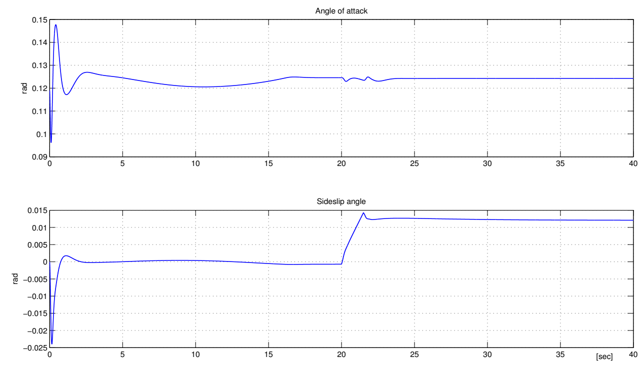

Fig. 6. The angle of attack α and the sideslip angle β.

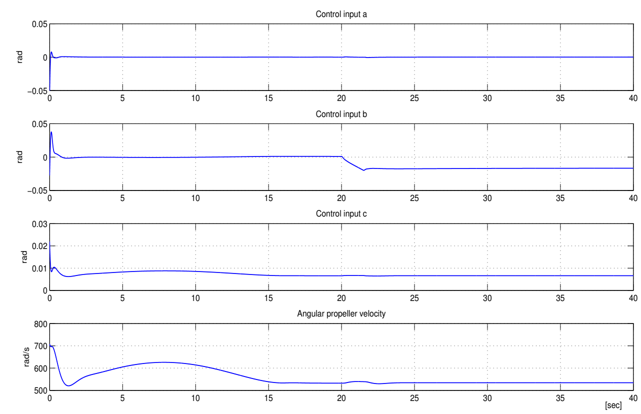

Fig. 7. The four control inputs a, b, c and $w_{\rm e}$.

works on this topic will be focused, besides others, on the problem of controlling in a robust way the transition of the aircraft between the hovering and fast forward flight configuration and on experimental validation of the proposed architecture.

REFERENCES

[1] P. Castillo, R. Lozano, and A. Dzul, *Modeling and Control of Mini Flying Machines*. Springer, 2003.

[2] L. Marconi and R. Naldi, "Nonlinear robust control of a reduced-complexity ducted mav for trajectory tracking," *44th IEEE Conf. Decision Control*, 2006.

[3] J. Pflimlin, P. Soures, and T. Hamel, "Hovering flight stabilization in wind gusts for ducted fan uav," *42nd IEEE Conf. on Decision and Control*, 2004.

[4] H. Schlichting and K. Gersten, *Boundary layer theory*. Springer, 1979.

[5] I. Guerrero, K. Londenberg, P. Gelhausen, and A. Myklebust, "A powered lift aerodynamic analysis for the design of ducted fan uavs," *2nd AIAA "Unmanned Unlimited" Systems, Technologies, and Operations*, 2003.

[6] E. Johnson and M. Turbe, "Modeling, control and flight testing of a small ducted fan aircraft," *AIAA Guidance, Navigation, and Control Conference and Exhibit*, 2005.

[7] R. Stengel, *Flight Dynamics*. Princeton University Press, 2004.

[8] B. Anderson and J. Moore, *Optimal Control: Linear Quadratic Methods*. Prentice Hall, 1990.

[9] K. Zhou, J. Doyle, and K. Glover, *Robust and Optimal Control*. Prentice Hall, 1995.